# Probing and Understanding Performances of Conductive Organic Radical Salts as Positive Electrode Material for anion-ion and dual-ion Batteries

Manon Mignon[a,c], Hugo Bevan[b], Jean-Noël Chotard[a,c,], Carine Davoisne,[a,c] Yann Le Gal[b], Olivier Jeannin[b], Dominique Lorcy*[b], Marc Fourmigué[b], Matthieu Becuwe*[a,c,]

**SUPPLEMENTARY INFORMATION**

**Table S1 Electrocrystallization conditions**

| X = $Br^-$, $BF_4^-$, $ClO_4^-$, $PF_6^-$, $AsF_6^-$ | $(TMTTF)_2Br$ | $(TMTTF)_2BF_4$ | | $(TMTTF)_2ClO_4$ | $(TMTTF)_2PF_6$ | $(TMTTF)_2AsF_6$ |
|---|---|---|---|---|---|---|
| TMTTF (mg, mmol) | 150, 0.57 | 150, 0.57 | 400, 1.54 | 400, 1.54 | 600, 2.3 | 150, 0.57 |
| TBAX (g, mmol) | 1.47, 4.56 | 2.87, 8.73 | 8.0, 24.3 | 8.0, 23.4 | 12.0, 31.0 | 3.77, 8.74 |
| TBAX (mmol) | 4.56 | 8.73 | 24.3 | 23.4 | 31.0 | 8.74 |
| I (µA) | 200 | 200 | 400 | 400 | 600 | 200 |
| $(TMTTF)_2X$ (mg) | 34 | 74 | 126 | 225 | 504 | 91 |
| Yield | 20% | 43% | 27% | 47% | 66% | 45% |

**Table S2 Chemical oxidation conditions for $(TMTTF)_2X$ synthesis**

| X = $BF_4^-$, $ClO_4^-$, $PF_6^-$ | $(TMTTF)_2BF_4$ | | $(TMTTF)_2ClO_4$ | $(TMTTF)_2PF_6$ |
|---|---|---|---|---|
| TMTTF (mg, mmol) | 100, 0.38 | 400, 1.54 | 100, 038 | 100, 0.38 |
| V $H_2O_2$ (µL) | 9.9, 96.0 | 39.6, 384.0 | 9.9, 96.0 | 9.9, 96.0 |
| V HX (µL, µmol) | 24.0, 192.0 | 95.6, 768.0 | 16.6, 192.0 | 28.3, 192.0 |
| V THF (mL) | 20 | 60 | 20 | 20 |
| **$(TMTTF)_2X$** (mg) | 30 | 255 | 60 | 18 |
| Yield | 25% | 54% | 51% | 14% |

**Table S3: Crystallographic data**

| | TMTTF | $(TMTTF)Br(H_2O)_2$ |
|---|---|---|
| CCDC deposit nb. | 2545862 | 2545863 |
| Formulae | C10 H12 S4 | $C_{10}H_{16}BrO_2S_4$ |
| FW ($g.mol^{-1}$) | 260.44 | 376.37 |
| System | monoclinic | monoclinic |
| Space group | C2/c | C2/m |
| $a$ (Å) | 15.773(2) | 16.6579(19) |
| $b$ (Å) | 5.9995(10) | 9.7456(11) |
| $c$ (Å) | 14.248(2) | 9.0958(10) |
| $\alpha$ (deg) | 90.00 | 90.00 |
| $\beta$ (deg) | 119.826(5) | 97.894(5) |
| $\gamma$ (deg) | 90.00 | 90.00 |
| $V$ ($Å^3$) | 1169.7(3) | 1462.6(3) |
| $T$ (K) | 150(2) | 150(2) |
| $Z$ | 4 | 4 |
| Cryst. dim. (mm) | 0.31×0.06×0.05 | 0.13×0.11×0.06 |
| $D_{calc}$ ($g.cm^{-3}$) | 1.479 | 1.709 |
| $\mu$ ($mm^{-1}$) | 0.77 | 3.369 |
| Absorption corr. | multi-scan | multi-scan |
| $T_{min}$, $T_{max}$ | 0.946, 0.962 | 0.4711, 0.7456 |
| Total refls | 4253 | 8455 |
| Uniq refls ($R_{int}$) | 1323 (0.0671) | 1772 (0.0268) |
| Uniq refls ($I > 2\sigma(I)$) | 1027 | 1638 |
| $R_1$, w$R_2$ | 0.0804, 0.1985 | 0.023, 0.063 |
| $R_1$, w$R_2$ (all data) | 0.0961, 0.2129 | 0.026, 0.0645 |
| GOF | 1.058 | 1.017 |

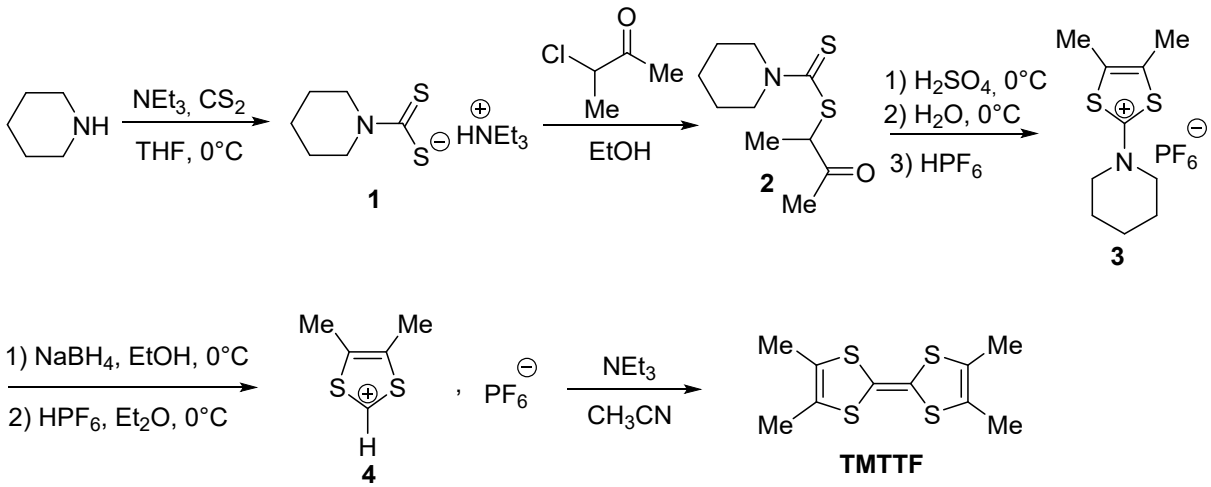


**Fig. S1: Synthetic pathway towards TMTTF**

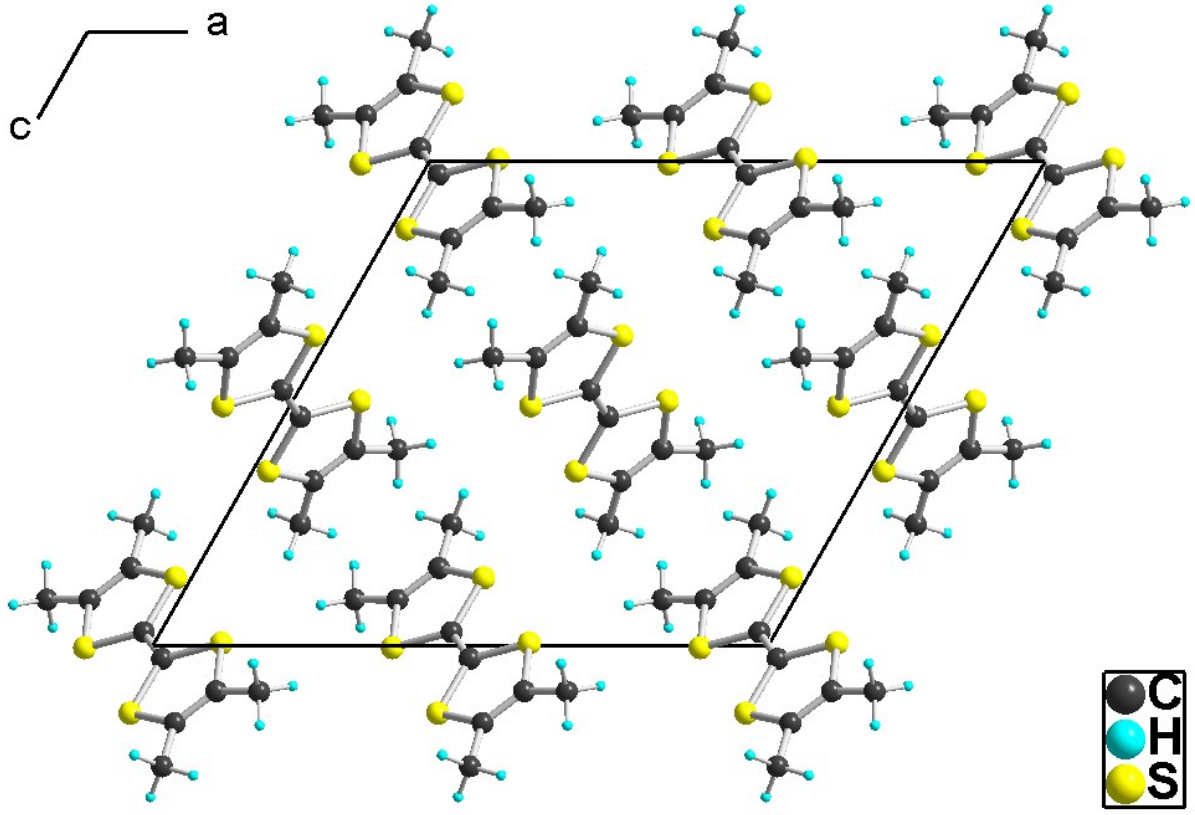


**Fig. S2: Projection view along the *b* axis of the unit cell of TMTTF (monoclinic phase)**

**Table S4: Evolutions of averaged intramolecular bond distances (a - d) in neutral TMTTF and its bromide salts**

| 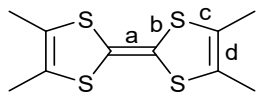 | a (Å) | b (Å) | c (Å) | d (Å) | T (K) | Ref. |
|---|---|---|---|---|---|---|
| $TMTTF^0$ | 1.359(2) | 1.763(2) | 1.767(3) | 1.343(2) | 120 | [1] |
| $TMTTF^0$ | 1.339(5) | 1.758(5) | 1.760(4) | 1.337(8) | 150 | this work |
| $TMTTF^+Br^-$ [(a)] Mol. A | 1.415(10) | 1.712(4) | 1.746(5) | 1.358(7) | RT | [2] |
| Mol. B | 1.394(10) | 1.717(4) | 1.740(6) | 1.336(7) | | |
| $TMTTF^+Br^-$ [(b)] | 1.394(5) | 1.720(2) | 1.738(4) | 1.350(2) | 150 | this work |

(a)In the salt formulated as (TMTTF)(Br)(PhCN)0.5(H2O)0.5; (b) In the newly reported salt formulated as $(TMTTF)Br(H2O)_2$

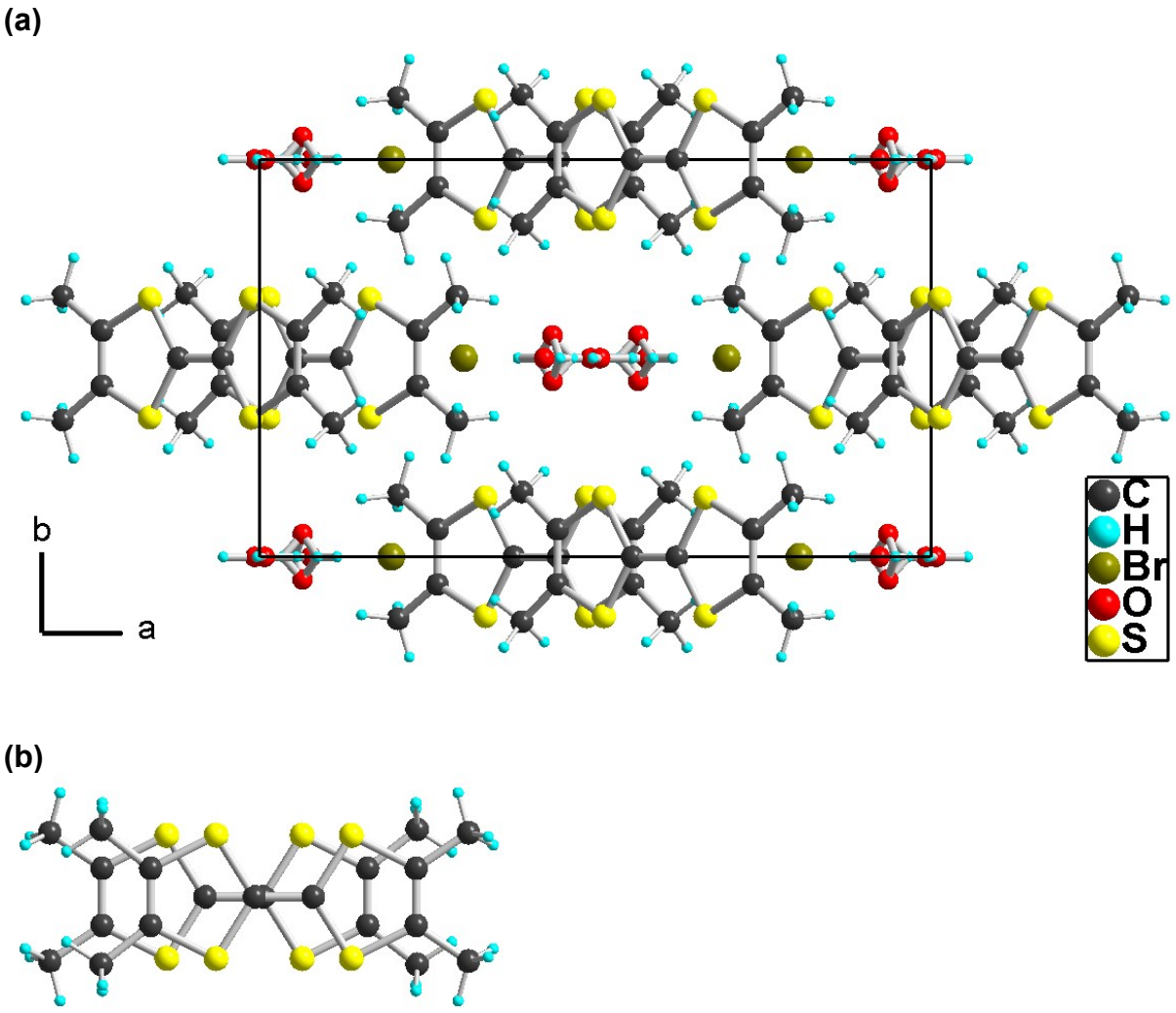


**Figure S3: Details of the crystal structure of (TMTTF)Br($H_2O$)$_2$ , (a) projection view of the unit cell along the *c* axis, and (b) intra-dimer bond-over-ring overlap**

**Table S5: Measured unit cell parameters of $(TMTTF)_2BF_4$, $(TMTTF)_2ClO_4$, $(TMTTF)_2PF_6$ and $(TMTTF)_2AsF_6$.**

| | $(TMTTF)_2BF_4$ | $(TMTTF)_2ClO_4$ | $(TMTTF)_2PF_6$ | $(TMTTF)_2AsF_6$ |
|---|---|---|---|---|
| Systeme and space group | Triclinic $P\bar{1}$ | Triclinic $P\bar{1}$ | Triclinic $P\bar{1}$ | Triclinic $P\bar{1}$ |
| T° | RT | RT | RT | RT |
| *a* (Å) | 7.11(8) | 7.13(4) | 7.15(4) | 7.1634(12) |
| *b* (Å) | 7.48(6) | 7.53(0) | 7.57(7) | 7.6095(11) |
| *c* (Å) | 12.94(4) | 13.015(8) | 13.21(1) | 13.2991(21) |
| *α* (°) | 85.46(8) | 84.40(4) | 82.58(5) | 81.9639(53) |
| *β* (°) | 85.97(3) | 85.23(9) | 84.62(4) | 84.1452(59) |
| *γ* (°) | 71.23(9) | 71.60(3) | 72.39(1) | 73.0613(55) |
| *V* (Å$^3$) | 650.38(2) | 6593.34(2) | 675.7(37) | 685.23(18) |

**Table S6: Unit cell parameters of, $(TMTTF)_2ClO_4$, $(TMTTF)_2BF_4$, $(TMTTF)_2PF_6$ and $(TMTTF)_2AsF_6$ as reported in literature.**

| | $(TMTTF)_2BF_4$ [3] | | $(TMTTF)_2ClO_4$ | $(TMTTF)_2PF_6$ | | $(TMTTF)_2AsF_6$ | |
|---|---|---|---|---|---|---|---|
| CCDC refcode | TMTFBF01 | TMTFBF10 | MTHFPC10[4] | MTHFPF[5] | MTHFPF01[6] | BUHGAM[7] | BUHGAM01[6] |
| System and space group | Triclinic $P\bar{1}$ | Triclinic $P\bar{1}$ | Triclinic $P\bar{1}$ | Triclinic $P\bar{1}$ | Triclinic $P\bar{1}$ | Triclinic $P\bar{1}$ | Triclinic $P\bar{1}$ |
| T° | 100 K | RT | RT | RT | 4 K | RT | 4 K |
| *a* (Å) | 6.97(1) | 7.112(3) | 7.115(3) | 7.650 | 6.936(5) | 7.178(4) | 6.898(5) |
| *b* (Å) | 7.49(1) | 7.468(3) | 7.515(2) | 13.23 | 7.508(4) | 7.610(3) | 7.553(3) |
| *c* (Å) | 12.89(2) | 12.946(3) | 12.992(3) | 7.14 | 13.045(5) | 13.317(4) | 13.166(5) |
| *α* (°) | 85.6(1) | 85.56(2) | 84.41(2) | 94.30 | 83.70(4) | 82.03(3) | 83.45(2) |
| *β* (°) | 93.2(1) | 94.05(2) | 85.27(2) | 108.75 | 87.20(3) | 95.75(3) | 87.20(3) |
| *γ* (°) | 110.1(1) | 108.80(4) | 71.53(3) | 83.15 | 70,81(5) | 107.11(3) | 70.73(3) |
| *V*(Å$^3$) | 629.77(163) | 648.196 | 654.78(38) | 678.885 | 637.66(65) | 687.168 | 643.25(60) |
| Plane-to-plane distance (Å) | 3.48 | | 3.51 | | 3.46 | | 3.45 |

**Table S7: Measured conductivity (S $cm^{-1}$) data on single crystals of $(TMTTF)_2X$ (X = $PF_6$, $ClO_4$, $AsF_6$, $BF_4$) along the *b* axis at ambient pressure using two-point probe methods compared with literature data (with four-point probe methods), both at room temperature.**

| **Material** | **Conductivity (S.$cm^{-1}$) (four-point measurements)** | **Conductivity (S.$cm^{-1}$) (two-point measurements)** |
|---|---|---|
| $(TMTTF)_2BF_4$ | 50 [8] | 3.47 [this work] |
| $(TMTTF)_2ClO_4$ | 30 [8] | 4.60 [this work] |
| $(TMTTF)_2PF_6$ | 20 [8] | 0.015 [this work] |
| $(TMTTF)_2AsF_6$ | 25 [9] | 1.75 [this work] |

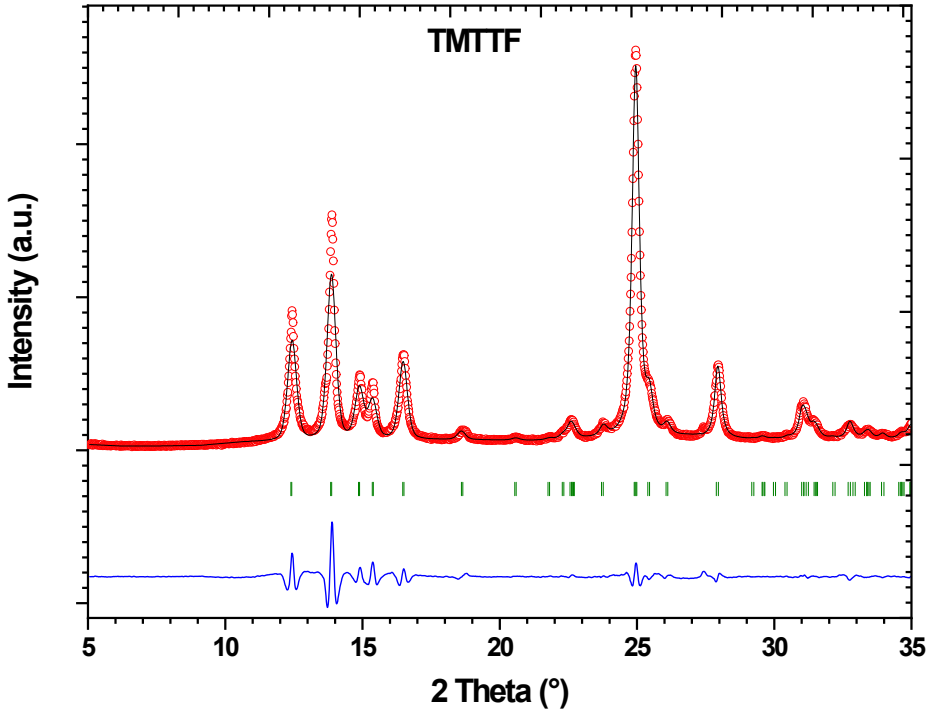


**Figure S4:** Rietveld refinement of TMTTF, the experimental data (red dots), calculated pattern (black line), Bragg positions (green markers) and difference curve (blue line).

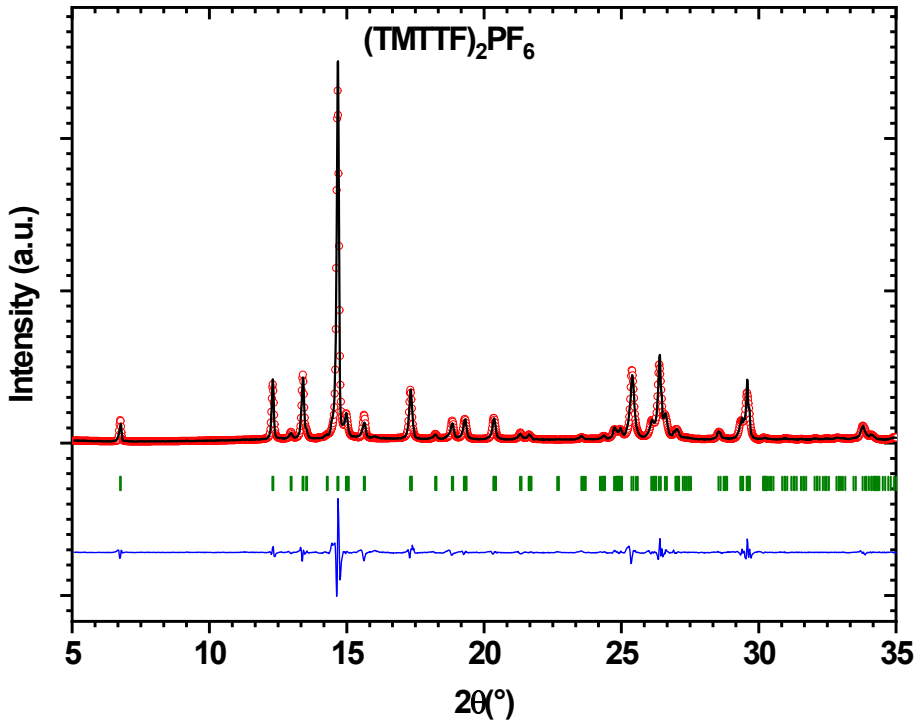


**Figure S5:** Rietveld refinement of $(TMTTF)_2PF_6$, the experimental data (red dots), calculated pattern (black line), Bragg positions (green markers) and difference curve (blue line).

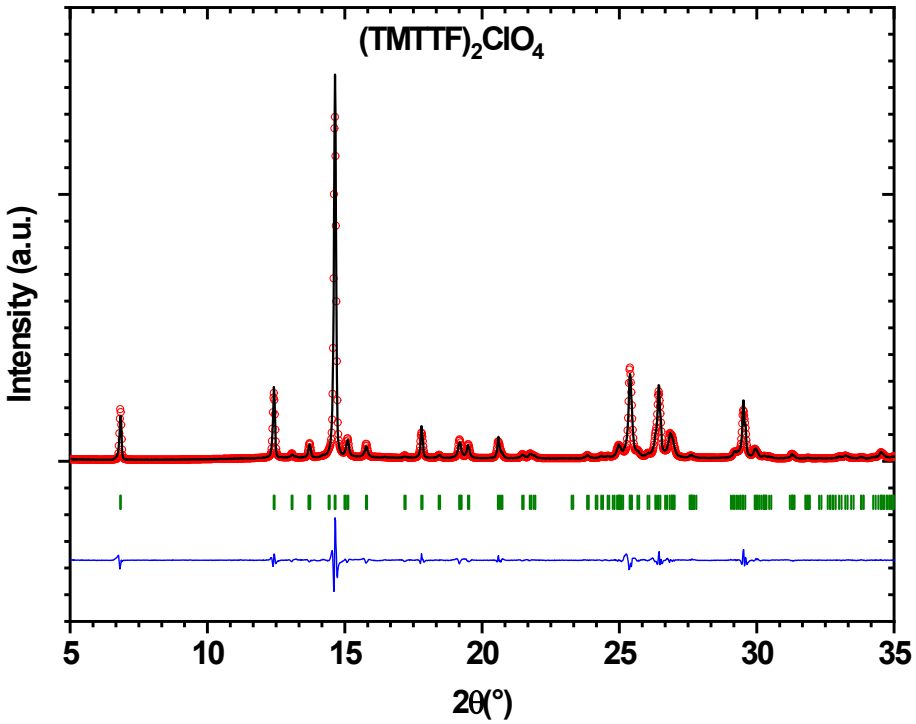


**Figure S6:** Rietveld refinement of $(TMTTF)_2ClO_4$, the experimental data (red dots), calculated pattern (black line), Bragg positions (green markers) and difference curve (blue line).

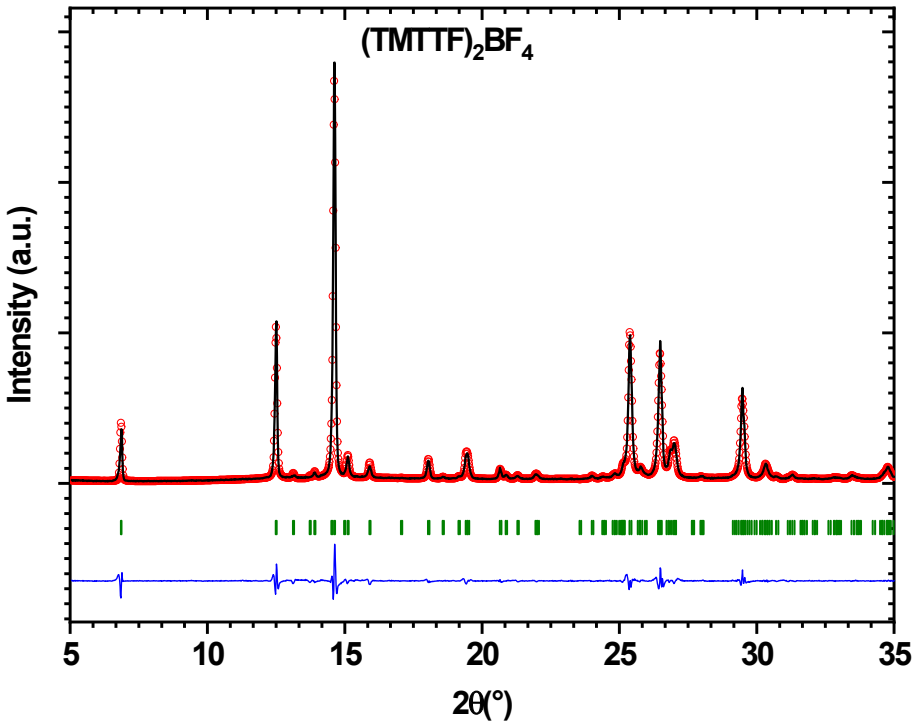


**Figure S7:** Rietveld refinement of $(TMTTF)_2BF_4$, the experimental data (red dots), calculated pattern (black line), Bragg positions (green markers) and difference curve (blue line).

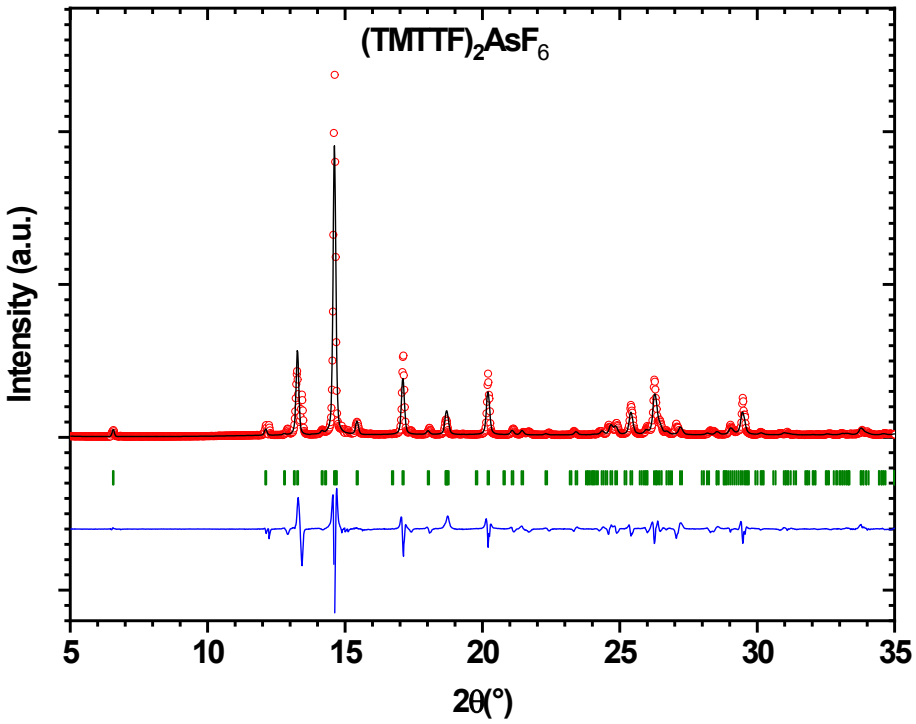


**Figure S8:** Rietveld refinement of $(TMTTF)_2AsF_6$, the experimental data (red dots), calculated pattern (black line), Bragg positions (green markers) and difference curve (blue line).

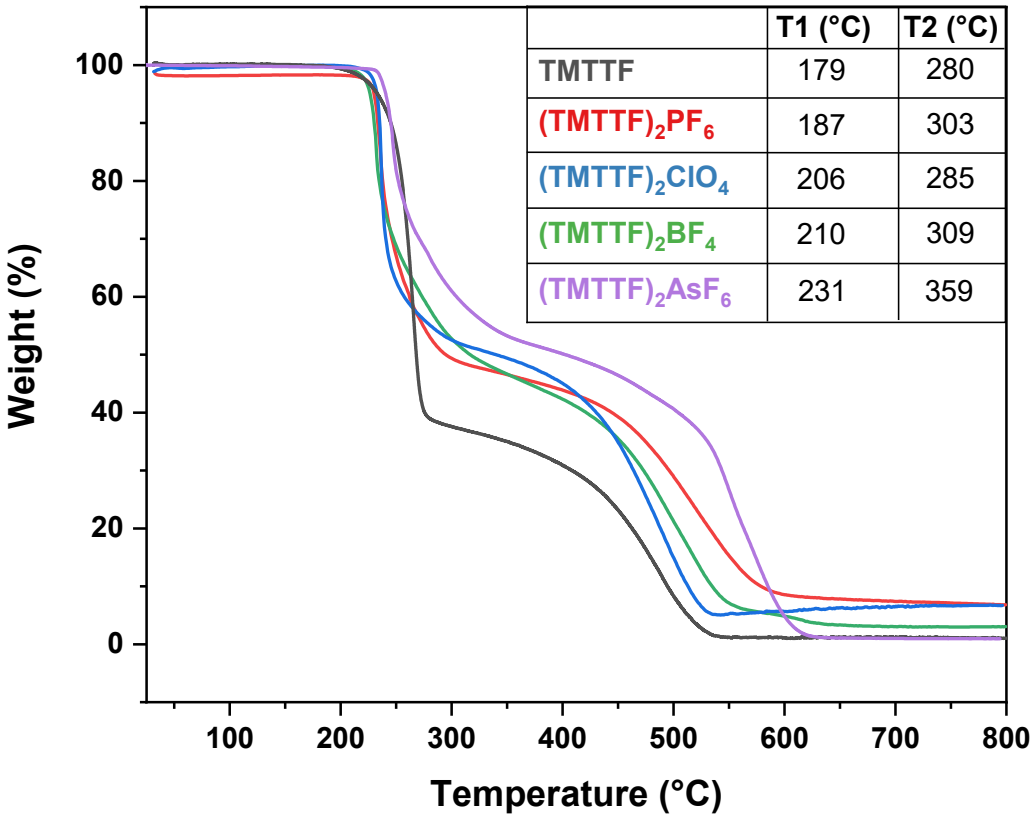


**Figure S9: Thermogravimetric analysis under air at 5°C.min$^{-1}$ with an input of the degradation temperature on TMTTF (grey) and radical salt associated with $PF_6^-$ (red), $ClO_4^-$ (blue), $BF_4^-$ (green) and $AsF_6^-$ (purple) anions.**

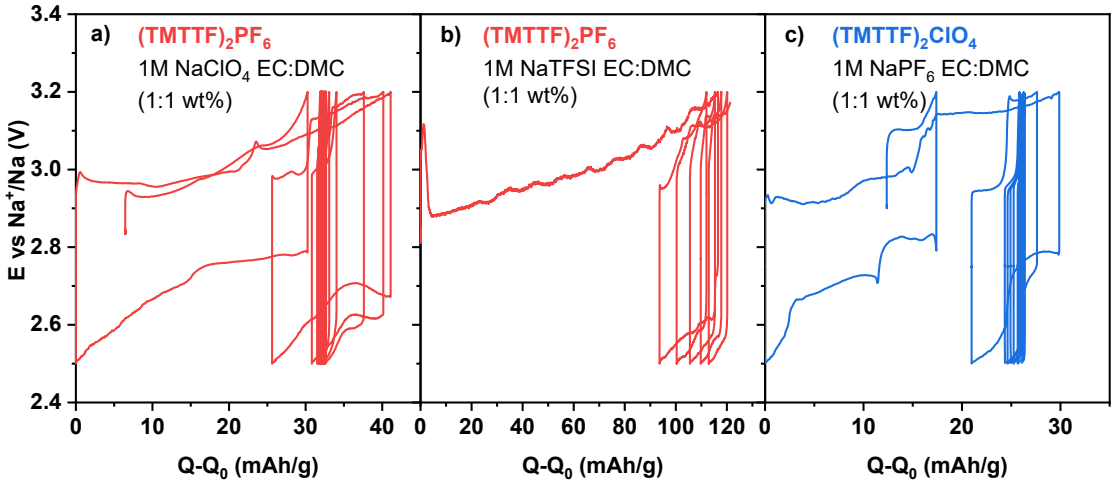


**Figure S10: Galvanostatic potential-composition profile of a) $(TMTTF)_2PF_6$ using 1M $NaClO_4$ EC:DMC (1:1 wt%), b) $(TMTTF)_2PF_6$ using 1M NaTFSI EC:DMC (1:1 wt%) and c) $(TMTTF)_2ClO_4$ using 1M $NaPF_6$ EC:DMC (1:1 wt%) as electrolyte. The electrode is mixed with 30 % of C45 cycled at C/10 between 2.4 and 3.2 V vs $Na^+/Na$.**

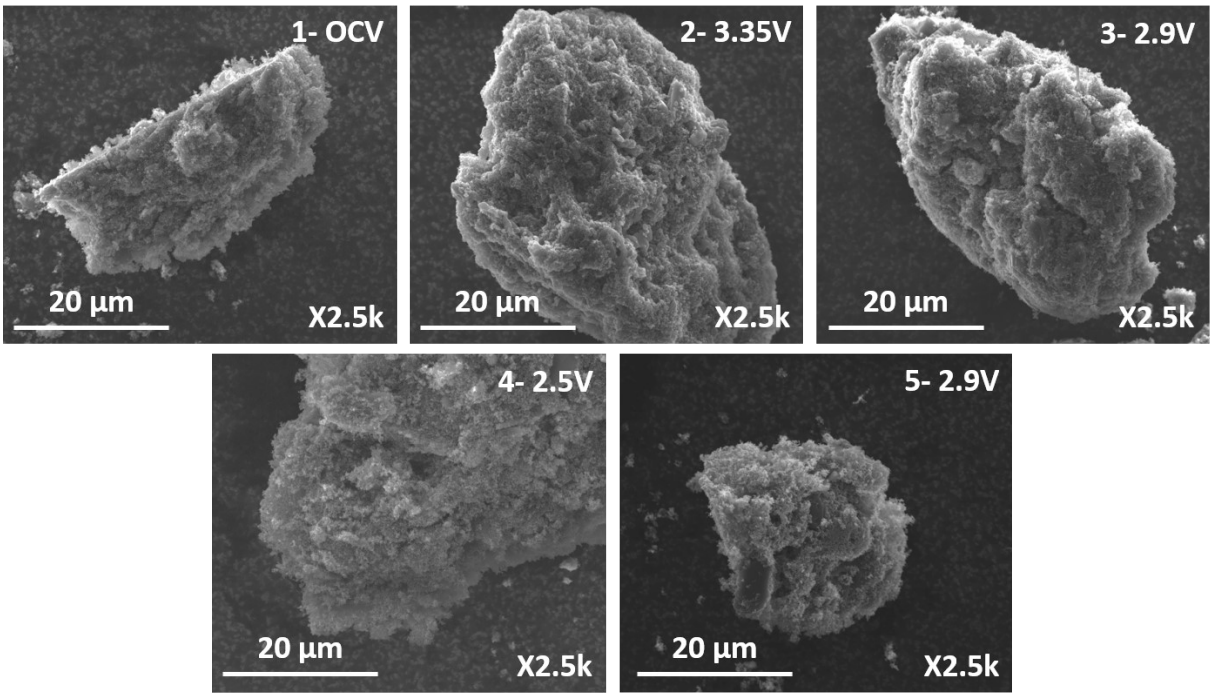


**Figure S11: *Ex situ* SEM characterisation of the $(TMTTF)_2PF_6$ electrode with 30 % of conductive carbon at different states of charge.**

Figure S12: XRD comparison between the initial material $(TMTTF)_2PF_6$, *in situ* measurement at 3.35V where $(TMTTF)PF_6$ is expected to form and simulated pattern of $(TMTTF)BF_4$.

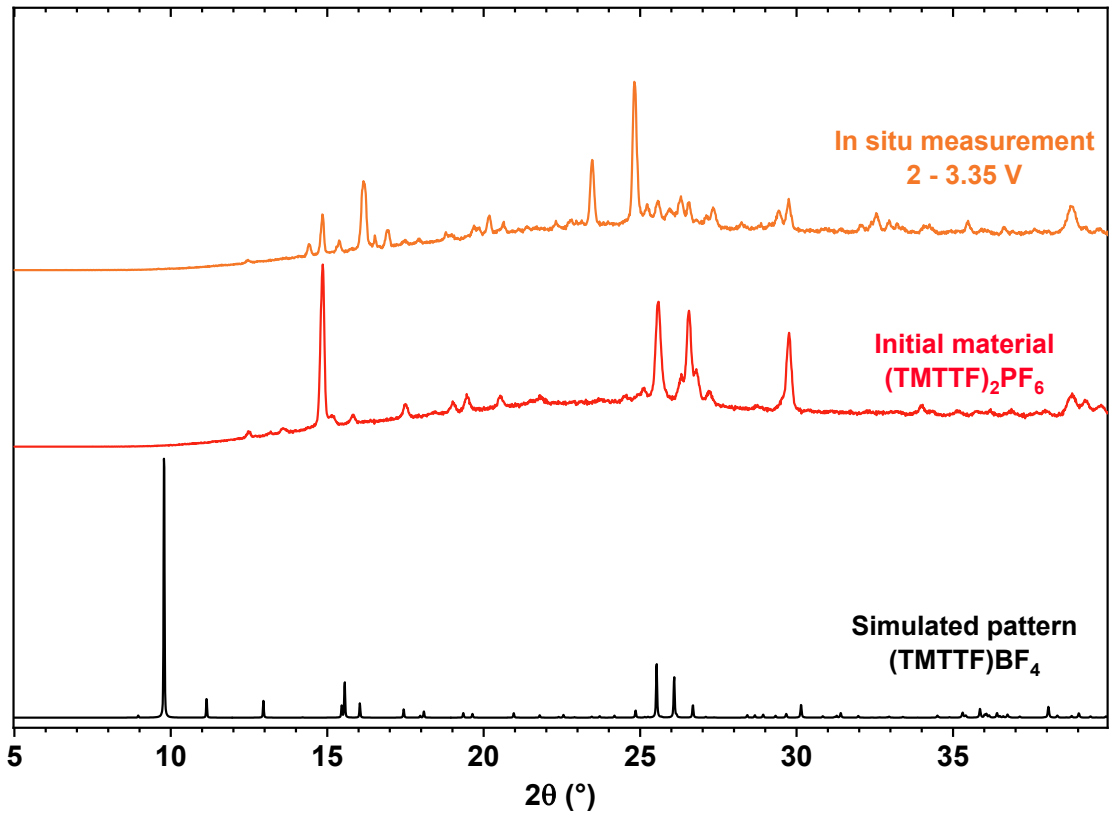

The CV of the TMTTF were performed in $CH_2Cl_2$ and in $CH_3CN$ using 0.1 M $Bu_4NPF_6$ as supporting electrolyte. Voltammograms were recorded at 0.1 V/s on a platinum electrode and the potentials were measured versus saturated calomel electrode (SCE)

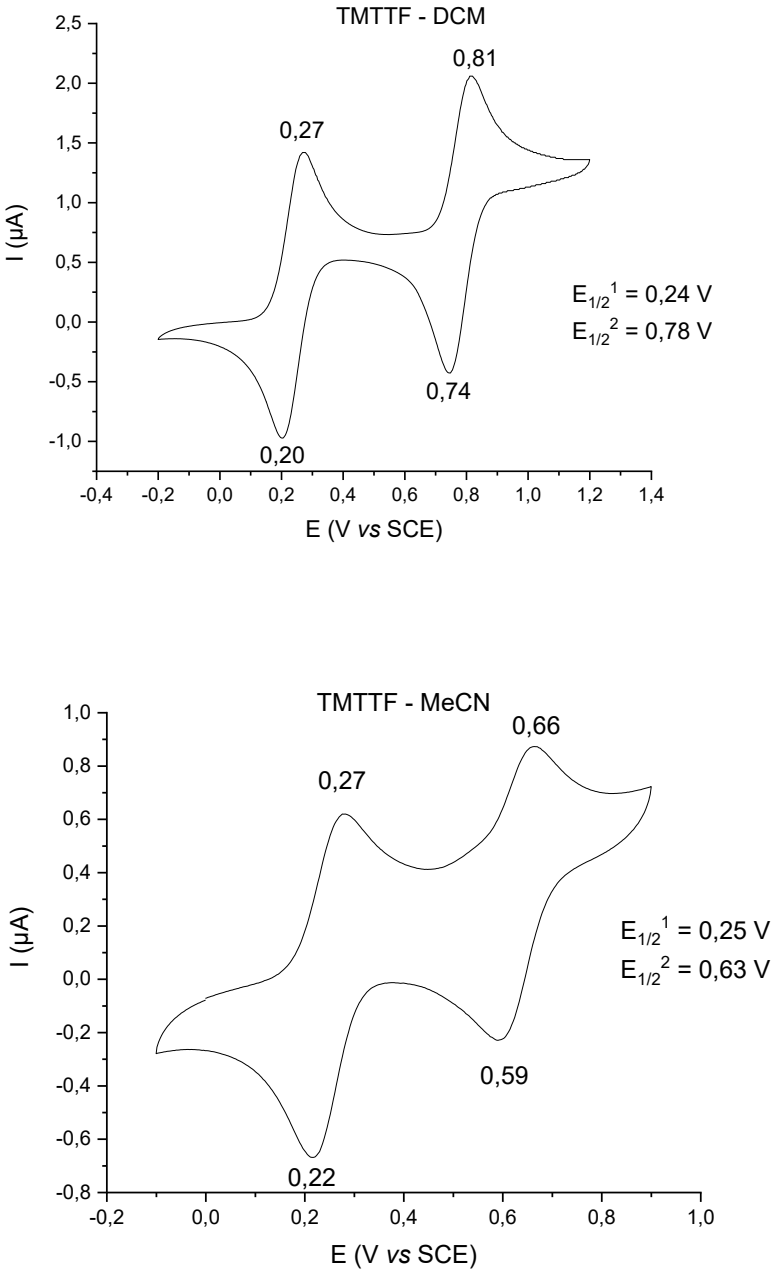


**Figure S13**: Cyclic voltammograms of TMTTF in $CH_2Cl_2$ (top) and in $CH_3CN$ (bottom) 0.1 M $NBu_4PF_6$ at 100 $mV.s^{-1}$

## References


[1] H. Mora, J. Fabre, L. Giral, et C. Montginoul, « Synthèses et caractérisation des dérivés méthylés du tétrathiafulvalène ; nouvelle voie d'accès au tétrathiafulvalène », *Bulletin des Sociétés Chimique Belges*, vol. 101, nº 2, p. 137-146, 1992.

[2] K. Honda, S. Takasaki, J.-I. Yamada, S.-I. Nakatsuji, et H. Anzai, « Tetramethyltetrathiafulvalenium Bromide Benzonitrile Water Solvate », *Acta Crystallogr C Cryst Struct Commun*, vol. 54, nº 2, p. 261-264, févr. 1998, doi: 10.1107/S0108270197013905.

[3] J. L. Galigné *et al.*, « Structure cristalline du fluoroborate de tétraméthyltétrathiafulvalène $(TMTTF)_2BF_4$ à 100 K et à température ambiante », *Acta Crystallogr B Struct Crystallogr Cryst Chem*, vol. 35, nº 5, p. 1129-1135, mai 1979, doi: 10.1107/S0567740879005720.

[4] B. Liautard, S. Peytavin, G. Brun, D. Chasseau, J. M. Fabre, et L. Giral, « Structure du di(tétraméthyltétrathiafulvalénium) perchlorate $[(TMTTF)_2ClO_4]$, $2C_{10}H_{12}S_{40},^{5+5+}.ClO_4^-$ », *Acta Crystallogr C Cryst Struct Commun*, vol. 40, nº 6, p. 1023-1026, juin 1984, doi: 10.1107/S010827018400665X.

[5] G. Brun *et al.*, « SELS DU RADICAL CATIONIQUE TMTTF (Tétraméthyltétrathiofulvalène). STRUCTURES ET PROPRIÉTÉS », *J. Phys. Colloques*, vol. 38, nº C7, p. C7-266-C7-269, déc. 1977, doi: 10.1051/jphyscol:1977751.

[6] T. Granier, B. Gallois, L. Ducasse, A. Fritsch, et A. Filhol, « 4 K crystallographic and electronic structures of $(TMTTF)_2X$ salts ($X^-$: $PF_6^-$, $AsF_6^-$ », *Synthetic Metals*, vol. 24, nº 4, p. 343-356, juin 1988, doi: 10.1016/0379-6779(88)90310-4.

[7] B. Liautard, S. Peytavin, G. Brun, et M. Maurin, *Crystal Structure Communications*, vol. 11, p. 1841, 1982.

[8] P. Delhaes *et al.*, « Physical Properties of One Dimensional Conductors », *Molecular Crystals and Liquid Crystals*, vol. 50, nº 1, p. 43-58, janv. 1979, doi: 10.1080/15421407908084413.

[9] R. Laversanne, C. Coulon, B. Gallois, J. P. Pouget, et R. Moret, « Structural and electrical properties of $(TMTTF)_2MF_6$ salts (M = P, As, Sb). Rôle of the anions », *J. Phyique Lett.*, vol. 45, nº 8, p. 393-399, 1984, doi: 10.1051/jphyslet:01984004508039300.